AN INDEPENDENT-FLOW-FIELD MODEL FOR A SDOF NONLINEAR STRUCTURAL SYSTEM, PART I: IDENTIFICATION AND COMPARISONS

Solomon C.S. Yim
e-mail: solomon.yim@oregonstate.edu

Huan Lin
e-mail: linh@engr.orst.edu

Ocean Engineering Program, Department of Civil Engineering
Oregon State University, OR 97331, U.S.A.

Abstract: *An independent-flow-field (IFF) model selected in this study to investigate the nonlinear response behavior of a medium-scale, experimental, submerged, moored structure is validated via parametric studies. Bifurcations in experimental responses are frequently observed and the associated nonlinear primary and secondary resonances are identified in frequency response diagrams. Distinct from previous investigations, this study intends to identify a set of "best-fit" constant coefficients for predictions and comparisons over the entire wave frequencies examined. It is concluded that the small-body, IFF model predicts reasonably well the nonlinear, moored and submerged structural response subjected to regular waves.*

Key Words: experimental, nonlinear, moored structure, comparison

Introduction

Complex nonlinear response phenomena of a submerged, moored ocean structural system subjected to periodic excitations, including nonharmonic responses, instability and sensitivity to initial conditions had been investigated in details [1-4]. Analytical predictions and numerical results indicated the existence of nonlinear responses including harmonic, sub-harmonic, super-harmonic and higher order nonlinear responses, even chaos.

Design of large-scale models incorporating nonlinear restoring forces and fluid-structure interactions in search of highly nonlinear responses may be difficult. Nonetheless, a medium-scale experiment investigating response behaviors of the submerged, moored structural system had been conducted [5]. Preliminary studies of such experimental results verified the existence of nonlinear characteristic responses (e.g. sub- and super-harmonics). Existence of an underlying bifurcation structure in the experimental responses was demonstrated in the corresponding frequency response diagram [6]. Coexistence of harmonic and sub-harmonic responses was also shown near secondary resonance [6].

A preliminary study of the experimental results had been carried out employing a simple, standard Morison (SM) type nonlinear model [7]. The geometric-nonlinear restoring force was approximated by two-term polynomials (linear and cubic) at static equilibrium. The wave-frequency dependency of the hydrodynamic properties was taken into account by identifying system parameters for each and every of the sample tests. Numerical predictions were in reasonably good agreement with experimental results. The authors, however, found from their numerical search results that there was no single set of constant parameters (coefficients) that would closely predict the response behavior over the entire frequency range of the experimental results considered. They recommended that an alternative model be developed and more detailed comparisons be performed [7].

In identifying a model to improve prediction capability of the experimental results, an investigation on modeling and parameter identification of the experiment had been recently carried out [8]. In their study, noisy experimental results near sub-harmonic resonance were used for identification with two nonlinear small-body hydrodynamic Morison type models chosen for comparison. The nonlinear restoring force of the proposed models, different from the previous standard Morison (SM) model, was approximated by a three-term polynomial (including an additional quadratic term) near dynamic equilibria, i.e. equilibria near the maxima of structural motions. Model predictions and experimental results were compared in both time and frequency domains. Numerical results indicated that the independent-flow-field (IFF) model with nonlinear-structure and nonlinear damping was the most suitable for the chosen experimental results. Feasibility of applying the IFF model with constant coefficients to the experimental results over the entire wave frequency range considered was yet to be assessed.

This two-part series study continues the investigation based on the small-body theory in examining the experimental response behaviors of the single-degree-of-freedom (SDOF) model subjected to regular waves. Knowing the frequency-dependency in the hydrodynamic properties, a major intent of the study is to identify a simple, nonlinear model with constant coefficients closely predicting and capturing complex, nonlinear structural response behavior in a periodic or nearly periodic fluid domain. The objectives of this paper (Part I) are threefold: 1) identify a "best" set of constant coefficients of the deterministic IFF model, 2) validate the model by comparing with experimental results, and 3) compare the predictions of the IFF model with those of the SM model in previous studies. With the validated IFF model, the companion paper (Part II) will investigate underlying intricate bifurcation patterns near resonances, and interpret complex nonlinear phenomena observed and discussed in previous studies.

The IFF model consists of an alternative form of Morison hydrodynamic damping (independent-flow-field), and a three-term-polynomial (including an additional quadratic term) approximation to the nonlinear restoring force. The IFF model employs a linear superposition of two independent flow fields separating the wave motion and the structural response. Response stability analysis is conducted by employing a harmonic balance method. System parameters suggested by Narayanan [8] identified in a noisy environment near sub-harmonic resonance are used in this study as initial estimates to further identify model parameters subjected to deterministic wave excitations with frequency over a much wider range. A “best” set of constant system parameters are later fine-tuned and identified based on extensive parametric studies and comparisons over the entire wave frequency range examined. Comparisons are conducted for all tests to assess the validity of the model, and representative samples are chosen for demonstration purpose. Causes for some “out-of-limit” responses observed in the experiment are inferred based on numerical results.

Experimental Model

While details of the experimental model and setup of a single-degree-of-freedom, hydrodynamically excited, submerged sphere moored by elastic mooring cables with geometric nonlinearity had been reported by Lin and Yim [7], for convenience of discussion, a brief description of the experiment is summarized in this section.

The experimental model considered is a geometrically nonlinear two-point moored single-degree-of-freedom (SDOF) system in surge. The models consist of a sphere on a steel rod supported by guyed masts six feet above the bottom of a closed wave channel (Fig. 1). The 18-inch diameter sphere, made of PVC, was virtually neutrally buoyant when submerged. Springs, with stiffness of 10 or 20 lb/ft, were horizontally attached to the sphere at angle of 60° or 90° to provide a nonlinear restoring force [5]. In this study, only the more nonlinear configuration (i.e. 90° or b=0 in Fig. 1) is investigated in detail to better demonstrate intrinsic nonlinear response characteristics. The restoring force, which contains a geometric nonlinearity, can be derived by a Lagrangian formulation [4]. The damping mechanism includes a linear system (structural) component (associated with the model connections and contact points of instrumentation), and a time-dependent coulomb friction component (due to a combination of hydrodynamic damping and the presence of the rod to refrain motion in surge). The coulomb friction originates from the lift force (in heave) and combined drag/lift moment (in pitch). The initial tension in the mooring cables varied from 15 to 30 lbs. depending on the test case. A majority of the tests were performed with relatively low initial tension (25 lbs.) to ensure nonlinear motion response [7].

Analytical Model

IFF Model

Employing the independent-flow-field (IFF) Morison damping and lumping the time-dependent coulomb friction into an equivalent linear system-damping coefficient, the equation of motion of the cable-moored system is given by [8]

$$M\ddot{x} + C_S\dot{x} + C'_D\dot{x}\left|\dot{x}\right| + R(x) = F_D(u) + F_I(\dot{u}, \ddot{x}) \tag{1}$$

where x and $\dot{x}$ denote the surge displacement and velocity, respectively; M, mass of sphere; R, nonlinear restoring force; C_S, effective (linear) system damping coefficient ($=\zeta_S C_{CR}$; ζ_S, damping ratio and C_{CR}, critical damping); C'_D , hydrodynamic damping coefficient; u, fluid particle velocity; F_D and F_I, drag and inertial components of the exciting force, respectively.

The nonlinear restoring force includes the force due to the mooring (R_M) and the force due to hydrostatic buoyancy (R_B). The spheres used in this experiment were virtually neutrally buoyant when submerged. Therefore, the forcing component caused by R_B was negligible and is not considered here

$$R(x) \cong R_M = K\left[4x + l_C\left(2b\frac{l_1 - l_2}{l_1 l_2} - 2x\frac{l_1 + l_2}{l_1 l_2}\right)\right] \tag{2}$$

where K is the spring constant, and b governs the spring configuration (Fig.1, b=0 for 90°), $l_{1,2}$ are the in-situ spring lengths, and l_C is the initial pre-tensioned spring length. It was found that 3-term polynomials, including a quadratic term, provide a good approximation to the restoring force near dynamic equilibria [8]

$$R(x) \cong k_1 x + k_2 x^2 + k_3 x^3 \tag{3}$$

The natural frequency T_n of the model is approximated near $\sqrt{\frac{k_1}{M}}$.

The exciting forces, consist of a Morison drag (F_D) and an inertial component (F_I) are, respectively, given by

$$F_D = \frac{\rho}{2} C_D A_P u|u| \tag{4}$$

and

$$F_I = \rho\forall(1 + C_A)\frac{\partial u}{\partial t} - \rho\forall C_A \ddot{x}, \tag{5}$$

where C_D is the hydrodynamic viscous drag coefficient; C_A, added mass coefficient; A_P, projected drag area; $\forall$, displaced volume; ρ, water density; and u, water particle velocity.

Wave-frequency dependency of the hydrodynamic parameters is noted in the previous studies, and identification of a simple, small body, nonlinear model with frequency-independent constant coefficients to capture the overall response behavior is attempted here. Extensive numerical simulations and comparisons with experimental results are conducted here to access the validity of the IFF model.

Parameters Identification

System parameters of the IFF model are first employed an initial estimates by Narayana based on a frequency domain identification technique on sample measurements of noisy sub-harmonic experimental test cases [8]. The initial estimates are later fine-tuned via comparisons with each and every experimental result in the time domain. A 'best' set of constant coefficients is hence identified (see Table 1), and with which the model predictions are consistent in good agreement with experimental results. Extensive parametric studies in response frequency diagrams will further validate the model with the set of parameters in later sections.

Stability Analysis

Employing the method of harmonic balance and solving the corresponding Hill's equation by applying the Floquet theory, the stability boundary of harmonic responses near resonances can be obtained (e.g. [1]). The stability boundaries near the primary resonance are given by

$$\omega^2 \approx k_1 + \frac{3}{2}k_3a^2 \pm \frac{3}{4}k_3a^2\sqrt{1-4\delta^2} \tag{6}$$

where a is the approximate response amplitude and δ the damping parameter.

The stability boundaries near the secondary sub-harmonic and super-harmonic resonances are, respectively, given by

$$\omega^2 \approx 4\left(k_1 + \frac{3}{2}k_3a^2\right) \pm 3k_3a^2\sqrt{1-4\delta^2} \tag{7}$$

and

$$\omega^2 \approx \frac{1}{4}\left(k_1 + \frac{3}{2}k_3a^2\right) \pm \frac{3}{16}k_3a^2\sqrt{1-4\delta^2} \tag{8}$$

Bifurcations and higher order nonlinear phenomena can be expected within the regions of instability.

Experimental Results

Tests Performed

Experimental tests conducted can be classified by two major categories as continuous search tests and data acquisition tests. The continuous search tests were intended to examine the overall behavior, and the acquisition tests record detailed information of model response under specified wave conditions. A brief description of each test category is reported as follows.

Continuous Search Tests -- Stability of the response of the nonlinear moored system subjected to periodic excitation can be predicted by referring to the backbone curve of the corresponding analytical model [4]. To identify qualitative changes in response, the sphere was subjected to waves with approximately constant amplitudes but with gradually varying frequencies. Note that because of wave generation limitations and designed wave conditions, the wave height could not be kept constant at all times. The wave height varied between 2.89 ft (0.47 Hz) and 0.37 ft (0.27Hz).

There were two search test runs performed on the 90° configuration. In the continuous search mode, the wave frequency was increased or decreased by 0.01 Hz every two to three minutes. In the first search test, the excitation frequency first increased from 0.10 Hz to 1.00 Hz and then investigated in the lower frequency range between 0.14 and 0.10 Hz. The second search test with specified wave frequencies of interest was intended to further examine the nonlinear phenomena observed previously. Both sub-harmonic and super-harmonic responses were frequently observed. A transitional phenomenon, e.g. from small-amplitude harmonic steady state to large-amplitude sub-harmonics also appeared in tests under the wave frequency near 0.5 Hz.

Data Acquisition Tests -- Data acquisition tests were performed to obtain steady-state responses with the results of the continuous search tests as a pre-cursor to identify nonlinear, sensitive regions. The length of the tests varied from 5 to 30 minutes to assure steady-state behaviors.

Observations

Resonances -- Relationship between wave excitation and response can be demonstrated via frequency response diagrams [9]. Figure 2 shows the characteristic frequency response based on the results of continuous search tests. Note that to maintain the sphere response sufficiently large for nonlinear behavior without damaging the model, both wave amplitude and frequency need to be accordingly maneuvered at the same time. Thus, the relationship between excitation and response should be depicted in a three-parameter space. The relationship can be demonstrated in a 2-D diagram by plotting the amplitude ratio (response amplitude/wave amplitude) against excitation frequency. Three possible resonances are indicated by the humps located near 0.13, 0.26, and 0.52 Hz, respectively (Fig.2). It is noted that nonlinear relationship between the response amplitude and wave amplitude is also embedded in the diagram presented. Also note that a conventional hydrodynamic presentation of amplitude-frequency relationship had been attempted using parameters of amplitude ratios vs. (wavelength × wave height). In such presentation, the underlying bifurcation structure was not clearly revealed. Therefore, the frequency response diagram is chosen for interpretations and comparisons throughout this study.

As shown in Fig.2, primary resonance is found to locate at near 0.26 Hz and secondary super-harmonic and sub-harmonic resonances are observed at near 0.13 Hz and 0.52 Hz, respectively. A jump phenomenon is observed at near the primary resonance where possible transitions of response stability are implied. Data-acquisition test D14 was hence performed with wave frequency at near 0.27 Hz (Fig.3). The wave amplitude was noticed transitioning from around 0.13 to 0.18 ft after around 200 seconds, and the response amplitude consequently increased from around 0.5 to 0.8 ft. The much more significant increase in the response amplitude compared to the variation in wave amplitude indicates a possible transition from a small-amplitude response state to a large-amplitude response. Co-existence of multiple responses is then implied. The response finally settles to the large-amplitude response mode, which indicates that between the two coexisting and competing response attractors, the larger-amplitude harmonics is of stronger stability [10].

The frequencies of secondary super-harmonic and sub-harmonic resonances, at around one-half (0.13 Hz) and two times (0.52 Hz), respectively, of that of the primary resonance (0.26 Hz) again verify the analytical prediction by Gottlieb et al. [6]. Transition from harmonic to super-harmonic response was first observed in the experiment at near 0.11 Hz and from super-harmonic to harmonic response at near 0.16 Hz. Stability boundaries are accordingly estimated (Fig.2). The system behavior within the wave frequency range of 0.11-0.16 Hz is super-harmonic.

Analytical predictions of stability boundaries based on Eqs.(6)-(8) are also shown in Fig.2 by solid lines. The analytical prediction, which clearly depicts the stability regions in the secondary resonances, however does not seem to be in line with the experimental results near the primary resonance. This may be due to the fact that in the ranges near the secondary resonances, the experimental wave height was kept near constant and the resulting amplitude-frequency relationship more closely follows the standard form (with fixed excitation amplitude). However, due to the limitation of the facility, notable (sometimes significant) variations in wave heights were observed in the frequency range near the primary resonance. As a result, the frequency response diagram presented is modified by a strong nonlinearity between wave and response amplitudes. Nonetheless, a jump (gap near 0.3 Hz) predicted by the analysis is present in the experimental results as noted.

Coexistence and Transitions -- Transitions to period doubling were observed in the experiment near the location of high frequency secondary resonance (0.52 Hz). Near the resonance, the system mostly behaves in the period-2 sub-harmonic fashion. To further the investigation in possible bifurcation cascades near the secondary sub-harmonic resonance, some data acquisition tests were performed. Figure 4b shows a sample structural response (Test D2) with wave frequency of 0.5 Hz. Transition is observed from a harmonic response state to another larger-amplitude harmonic state and then a steady-state sub-harmonic response. Two distinct harmonic and a sub-harmonic response attractors are hence indicated to coexist near the sub-harmonic resonance as analytically predicted by Gottlieb and Yim [4]. The transition is possibly induced by tank noise as previously indicated, and the sub-harmonics are assessed to have the relatively stronger stability [10].

Large Amplitude Motion -- It is also observed in the search test when the wave frequency is near 0.27 Hz, the sphere is excited into a very large-amplitude motion. The amplitude that the sphere tends to reach is beyond the limitations of the mechanical configuration such that the wires connecting the sphere and springs were dislodged from the pulleys, and the data collection was terminated [5]. The cause for such an amplitude jump, which has not been discussed in previous studies, is investigated here.

Comparisons Between Predictions and Experimental Results

Detailed comparisons of experimental results and numerical predictions are illustrated in the frequency response diagram and time domain in this section.

Frequency Response Diagram

Comparisons of simulations of the IFF model with experimental results are shown in Fig.5, where experimental results are denoted by "o" and simulations by "+". The simulations are steady-state solutions from the analytical model (Eq.(1)) subjected to the measured wave excitations with 50 initial conditions varied from (-7 ft, -7 ft/s) to (7 ft, 7 ft/s).

It is observed that the IFF model simulations match well with the measured results in amplitude and characteristics over the frequency range examined (Fig.5). Primary resonance near 0.26 Hz and secondary resonances near 0.13 and 0.52 Hz, respectively, are closely simulated. Coexisting harmonic and sub-harmonic responses near 0.5 Hz in the experimental results are also clearly demonstrated. The simulated solutions also indicate the potential existence of "very-large-amplitude" harmonic responses in the frequency range of [0.25 0.53] Hz. The coexisting large-amplitude responses are resulted from large initial conditions. Most of the experimental search runs started with the quiescent initial conditions, and the model response mostly follows the lower (smaller amplitude) response curve. The "very-large-amplitude" responses are out of the limitation of the designed mechanical configuration of the experiment, and cannot be realized in the test runs. However, for some tests at wave frequency near 0.27 Hz, the sphere was led to such a large amplitude level that the strings connecting the springs and sphere popped off the pulleys, and consequently the test was terminated. The tendency of reaching the "very-large-amplitude" motions may be a result of perturbation-induced transitions. With the presence of perturbations (tank noise and wave amplitude variations in this experiment), the sphere was driven to the higher response curve (larger amplitude) beyond the limitation of the experimental configuration. The reaching of very-large-amplitude response leads to the strings popping out of the pulleys. The good agreement between the predictions and measured data however, suggests the applicability of the small body theory to describe and predict the model response behavior.

Compared to previous studies [6,7], the IFF model clearly shows significant improvements in simulation and prediction of experimental responses, especially near super- and sub-harmonic resonances. The simulation results also provide a complete depiction of the global behavior of the system.

Time History

Data acquisition tests are conducted at wave frequency near resonances, namely, 0.13, 0.26 and 0.52 Hz for detailed examination of more "nonlinear" and "sensitive" responses observed in the search test. Model simulations are intended to match the experimental results in amplitude and characteristics, and also to determine possible causes for transitional phenomena, e.g. from small-amplitude harmonics to large amplitude harmonics as shown Fig.3 and from harmonics to sub-harmonics as shown in Fig.4.

Comparison of numerical predictions and experimental results of coexisting two distinct harmonic responses at wave frequency of 0.27 Hz (Test D14) is shown in Fig. 6 (cf. Fig.3). An example of transition from small-amplitude harmonics to large-amplitude harmonics in Test D14 is noted in Fig.3b. The transition at around the 150^{th} second is possibly caused by the variation in wave height from around "0.25 " ft to "0.33 " ft as shown in Fig.3a. The amplitude-variation caused transition is verified by numerical results in the frequency response diagram (cf. Fig.5). Numerical results confirm and assimilate the coexistence of small-amplitude and large-amplitude harmonics near the primary resonance.

Comparison of numerical predictions and experimental results of coexisting harmonic and sub-harmonic responses at wave frequency of 0.50 Hz (Test D2) is shown in Fig. 7 (cf. Fig.4). A transition from a small-amplitude harmonics to large-amplitude sub-harmonics in Test D2 is noted in Fig.4b. The transition at around the 80^{th} to 120^{th} second is possibly caused by the variation in wave height from around "1.5 " ft to "2.4 " ft as shown in Fig.4a. The amplitude-variation caused transition is verified by numerical results in the frequency response diagram (cf. Fig.5). It shows the multiple coexistence, near the secondary resonance of small-amplitude harmonics, sub-harmonics and large-amplitude harmonics, depending on wave amplitude and initial conditions. With quiescent initial conditions, when the wave amplitude increases, the structural response may transition from small-amplitude harmonics to sub-harmonics or even large-amplitude harmonics. With fixed wave height, when the initial conditions are larger, the transition in response stability may also occur. The coexisting very large-amplitude harmonic response might be experimentally realized when the experiment scale is sufficiently large.

Comparison of the simulation and super-harmonic experimental result at wave frequency of 0.13 Hz (Test D3) is shown in Fig. 8. The numerical results indicate there exists only one response attractor at the frequency. Good agreement in characteristics and amplitude is observed between the experimental and numerical results as shown in Fig.8b.

Concluding Remarks

The validity and prediction capability of an IFF, small-body model with constant system parameters simulating a medium-scale nonlinear moored structural experiment are assessed in this study. Based on the results presented here, the following concluding remarks are offered:

1. The IFF model has been shown here to provide significant improvements in response prediction capability when compared to similar SDOF models considered in previous studies.
2. Numerical simulations are in good agreement with experimental results in both overall behavior and individual response trajectories. The good agreement validates the IFF model as well as verifies the applicability of the small body theory for the experimental results considered.
3. Simulations of the frequency response diagram capture the resonances, jump phenomenon and coexistence as exhibited in the experimental results. Good agreement between simulations and experimental results is also shown through time history in

response characteristics and amplitude.

4. Numerical simulations also indicate the existence of very-large-amplitude harmonic responses. Under the perturbations of tank noise and wave amplitude variation, the sphere is sometimes driven to this response attractor, leading to large amplitude motions observed in the experiment.

5. Experimentally observed transition phenomena, e.g. from small-amplitude harmonics to large-amplitude harmonics and from harmonics to sub-harmonics, are also numerically simulated. The coexisting response attractors and their possible interactions and transitions are identified based on the frequency response diagram from the simulations.

Acknowledgments

Financial support from the United State Office of Naval Research Grant No. N00014-92-1221 is gratefully acknowledged.

References

[1] Virgin, L.N., and Bishop, S.R., 1988, "Complex dynamics and chaotic responses in the time domain simulations of a floating structure," *Ocean Engrng*, **15**, pp. 7-90.

[2] Thompson, J.M.T., 1989, "Chaotic phenomena triggering the escape from a potential well," *Proc. Roy. Soc. London,* **A421**, pp. 195-225.

[3] Soliman, M., and Thompson, J.M.T., 1991, "Transition and steady state analysis of capsize phenomena," *Appl. Ocean Res.*, **13**, pp. 82-92.

[4] Gottlieb, O., and Yim, S.C.S., 1992, "Nonlinear oscillations, bifurcations and chaos in a multi-point mooring system with a geometric nonlinearity," *Appl. Ocean Res.*, **14**, pp. 241-257.

[5] Yim, S.C.S., Myrum, M.A., Gottlieb, O., Lin, H., and Shih, I-M, 1993, *Summary and Preliminary Analysis of Nonlinear Oscillations in a Submerged Mooring System Experiment*, Ocean Engineering Report No. OE-93-03, Oregon State University.

[6] Gottlieb, O., Yim, S.C.S., and Lin, H., 1997, "Analysis of bifurcation superstructure of a nonlinear ocean system," *J. Engng. Mech., ASCE*, **123**, pp. 1180-1187.

[7] Lin H., and Yim, S.C.S., 1998, "Experimental calibration of bifurcation superstructure of nonlinear system," *J. Engng. Mech., ASCE*, **124**, pp. 471-475.

[8] Narayanan, S., 1999, "Experimental analysis of a nonlinear moored structure," Ph.D. Thesis, Civil Engineering Department, Oregon State University.

[9] Nayfeh, A.H., and Mook, D.T., 1979, *Nonlinear Oscillations.* New York: Wiley & Sons.

[10] Lin, H., and Yim, S.C.S., 1995, "Chaotic roll motion and capsizing of ships under periodic excitation with random noise," *Appl. Ocean Res.*, **17**, pp. 185-204.

C_A	C_D	k_1(lb/ft)	k_2 (lb/ft^2)	k_3 (lb/ft^3)	C'_D	ζ_S
0.25	0.1	9.3	4.0	4.0	0.02	6%

Table 1 The 'best' set of constant coefficients of IFF model

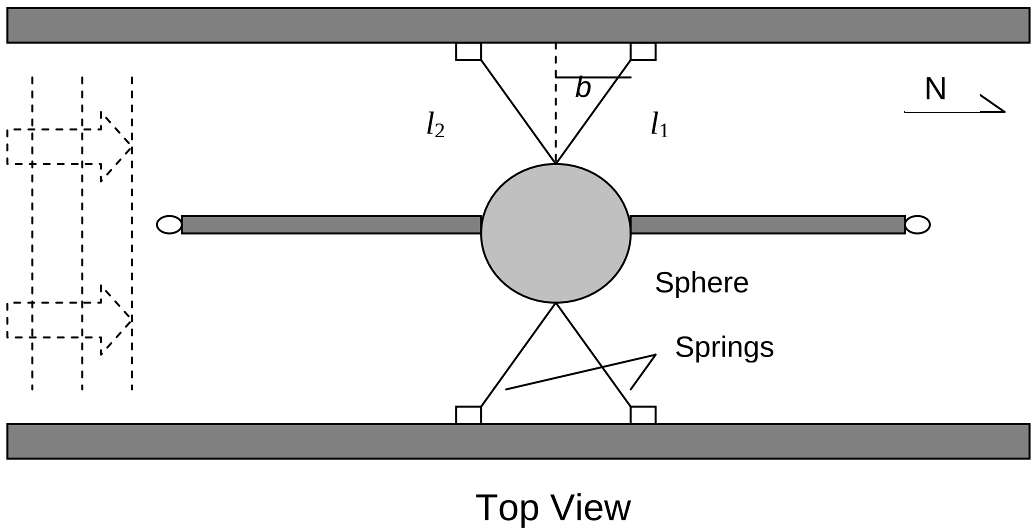

Fig.1 Experimental model of a submerged, hydrodynamically damped and excited nonlinear structural system

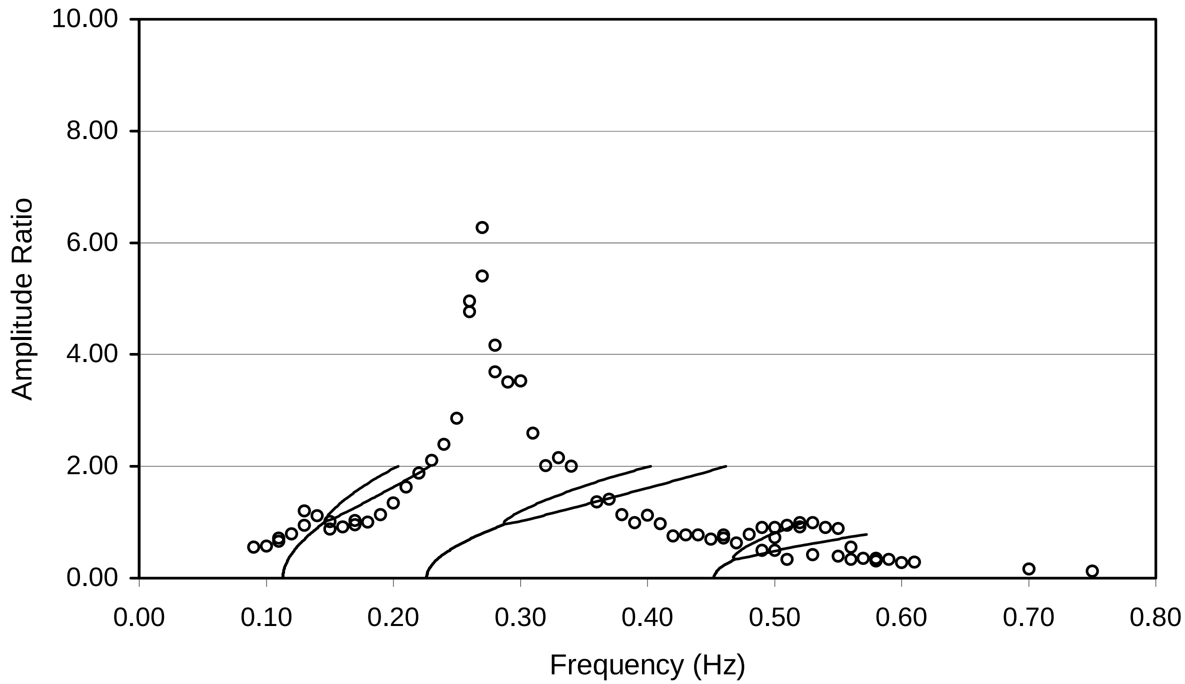

Fig. 2 Comparison of experimental results (‘o’) and analytical prediction (‘—’) in normalized frequency response diagram; C_A =0.25, C_D =0.1, k_1 =9.3 (lb/ft), k_2 =4.0 (lb/ft^2), k_3 =4.0 (1b/ft^3), C'_D =0.02, and ζ_S =6%

a)

b)

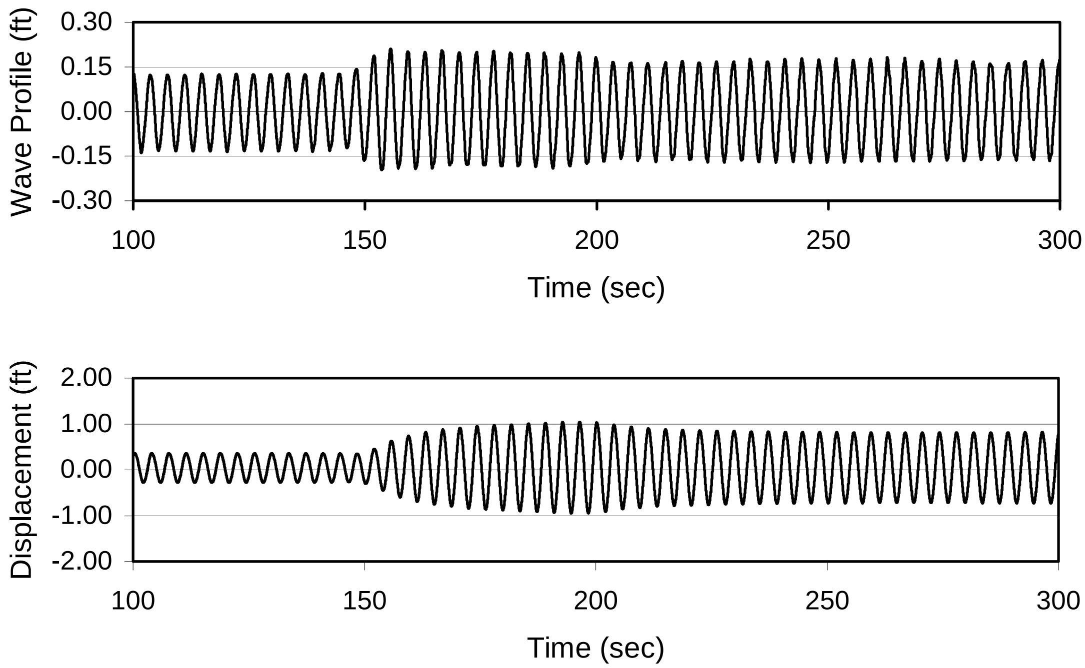

Fig. 3 Transition from small-amplitude harmonics to large-amplitude harmonics at wave frequency of 0.27 Hz (Test D14); a) wave profile, and b) sphere displacement

a)

b)

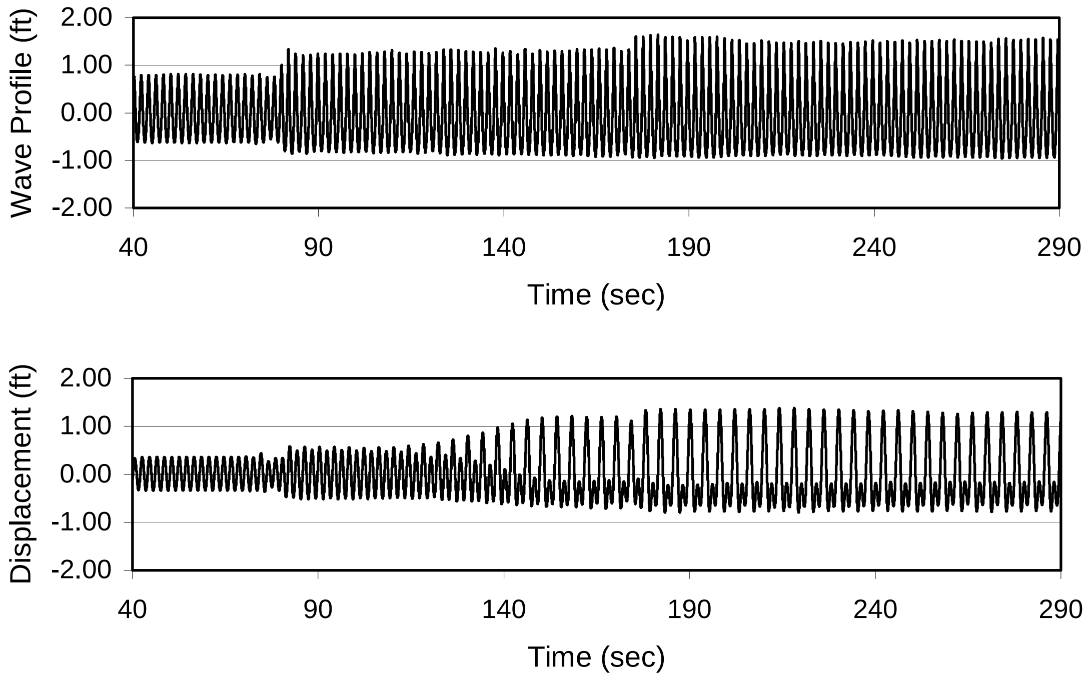

Fig. 4 Transition from harmonic response (0.5 Hz) to sub-harmonic response (0.25 Hz) at wave frequency of 0.5 Hz (Test D2); a) wave profile, and b) sphere displacement

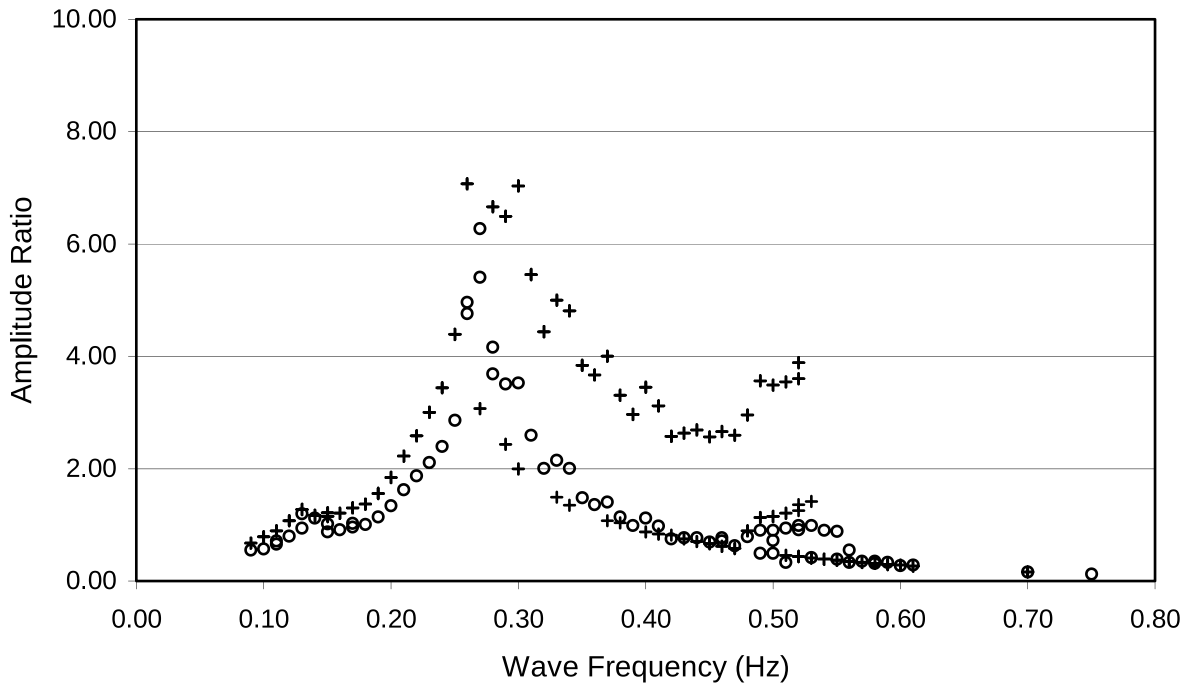

Fig. 5 Comparisons of experimental results ('o') and IFF model predictions ('+') in normalized frequency response diagram; C_A =0.25, C_D =0.1, k_1 =9.3 (lb/ft), k_2 =4.0 (lb/ft^2), k_3 =4.0 (1b/ft^3), C'_D =0.02, and ζ_S =6%

a)

b)

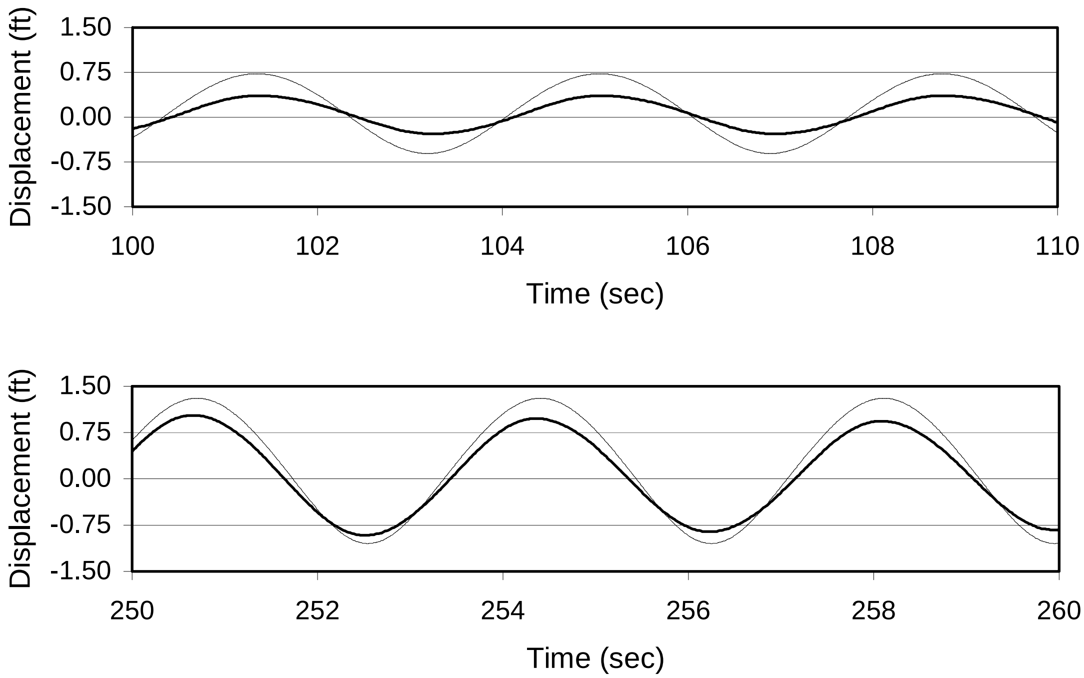

Fig. 6 Coexisting responses near primary resonance at wave frequency of wave frequency of 0.27 Hz (Test D14); a) small-amplitude harmonics, and b) large-amplitude harmonics; experimental results – solid lines and simulations – dashed lines

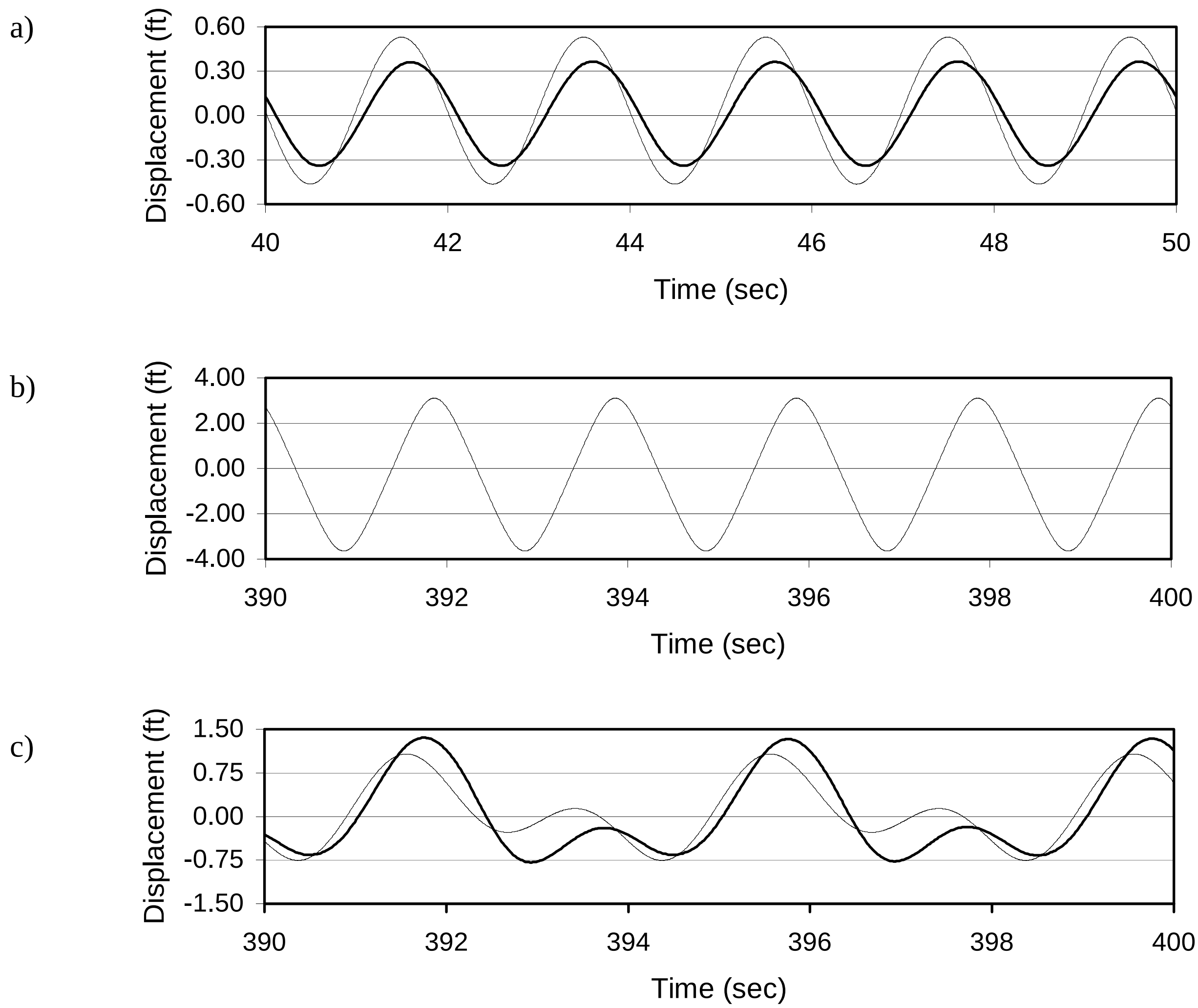

Fig. 7 Coexisting responses near sub-harmonic resonance at wave frequency of 0.5 Hz (Test D2); a) small-amplitude harmonics, b) sub-harmonics (experimental results – solid lines, simulations – dashed lines), and c) large-amplitude harmonics (simulation)

a)

b)

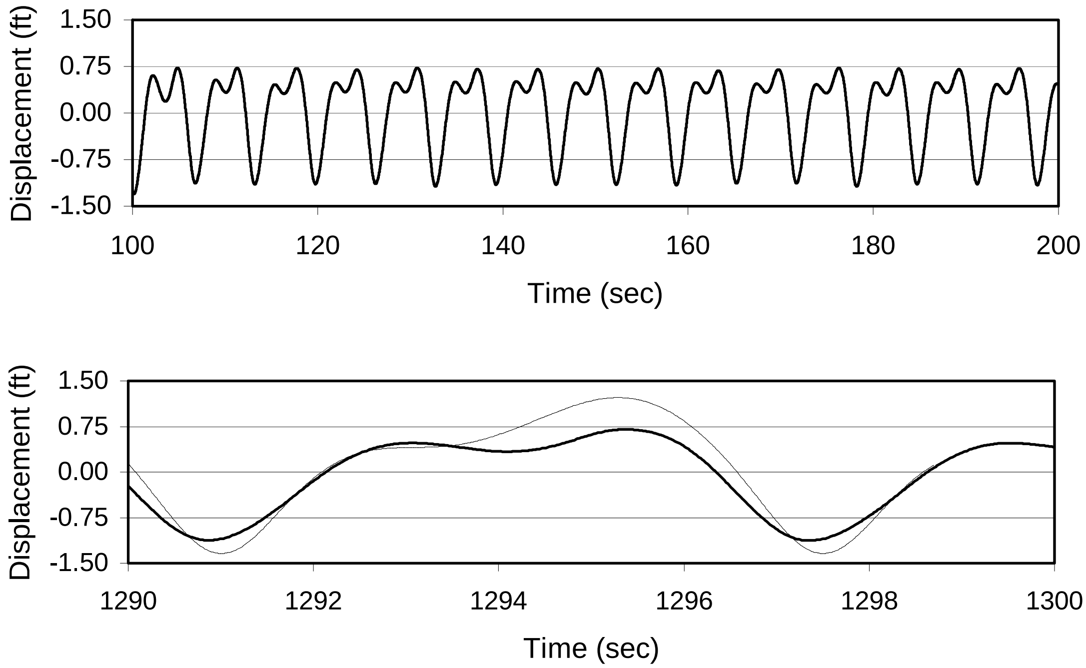

Fig. 8 Comparison of super-harmonic response at wave frequency of 0.13 Hz; a) experimental result (Test D3), and b) comparison (experimental – solid line, simulated – dashed line)